

# Magnetic and transport properties of amorphous $Gd_xGe_{1-x}$ alloys near the metal-insulator transition

E. Helgren\* and F. Hellman

*Department of Physics, University of California Berkeley, Berkeley, California 94720, USA*

Li Zeng†

*Material Science Program, University of California, San Diego, La Jolla, California 92093, USA*

N. Sinenian

*Department of Physics, University of California, San Diego, La Jolla, California 92093, USA*

R. Islam

*Center for Solid State Science, Arizona State University, Tempe, Arizona 85287, USA*

David J. Smith

*Department of Physics and School of Materials, Arizona State University, Tempe, Arizona 85287, USA*

(Received 2 July 2007; published 28 November 2007)

The temperature and field dependence of magnetization and conductivity of amorphous Ge doped with Gd ( $a$ - $Gd_xGe_{1-x}$ ) has been measured for a wide range of  $x$  ( $0.08 < x < 0.25$ ) near the metal-insulator transition. Magnetization and magnetic susceptibility measurements show strong magnetic interactions and a low temperature spin-glass freezing. High field magnetization and susceptibility per Gd atom in the paramagnetic state are significantly suppressed below that of noninteracting Gd, as observed previously for  $a$ -Gd-Si alloys. However, unlike  $a$ -Gd-Si, the low field susceptibility does not fit a Curie-Weiss law and shows no significant dependence on composition. Conductivity measurements show that Gd causes localization of charge carriers below a characteristic temperature  $T^*$ , which also marks the onset of significant negative magnetoresistance. Both  $T^*$  and the magnitude of the MR are significantly lower in  $a$ -Gd-Ge than in comparable  $a$ -Gd-Si alloys. It is proposed that the large effects of the host matrix (Ge vs Si) are due to differences in both the band gap and dielectric constant, which cause changes in screening, thereby altering the effect of Gd magnetic moments on the localization of carriers and on the indirect mediated Gd-Gd exchange interactions.

DOI: [10.1103/PhysRevB.76.184440](https://doi.org/10.1103/PhysRevB.76.184440)

PACS number(s): 75.50.Pp, 71.23.Cq, 75.20.Hr, 71.30.+h

## I. INTRODUCTION

The introduction of magnetic moments into semiconducting matrices has revealed a rich spectrum of magnetic, transport, tunneling, and thermodynamic properties. Most studies have focused on crystalline systems, such as GaMnAs and other dilute magnetic semiconductors<sup>1,2</sup> (DMS) and semiconducting oxides doped with transition metals [primarily Co (Refs. 3 and 4)]. These materials are important both for what they reveal about electron transport in the presence of magnetic moments, typically resulting in strong electron correlation effects, and for their potential technological significance, due to their possible application in quantum computing schemes or as a source for spin-injected current.<sup>5</sup> Studies of amorphous Si ( $a$ -Si) with magnetic dopants (particularly Gd) have revealed remarkable properties, with the most dramatic effects showing up close to the metal-insulator transition (MIT). Many of the observed phenomena, such as extremely large negative magnetoresistance (MR) at low temperatures, magnetic field-induced changes in the electron density of states, and the loss of significant spectral weight to high energy seen in IR absorption, indicate strong coupling of the electronic and magnetic moments as well as electron-electron correlation effects.

The results for  $a$ -Gd-Si are reminiscent of results reported for the much-studied manganites as well as the DMS mate-

rials. However, significant differences are clearly evident in these various systems. Both the DMS and perovskites are usually crystalline, and the more concentrated systems studied in recent years such as GaMnAs and the manganites are commonly ferromagnetic with large MR effects near their Curie temperatures  $T_C$ . In contrast,  $a$ -Gd-Si has strong but frustrated interactions, leading to spin-glass freezing at low temperatures and MR, even at moderately high temperature  $T$  (1% at 90 K), which grows exponentially with decreasing  $T$  for alloys on both sides of the MIT.

The introduction of magnetic ions into both crystalline systems (e.g., GaMnAs) and the  $a$ -Gd-Si and  $a$ -Gd-Ge amorphous alloys discussed here adds charge carriers, which, in turn, influence the magnetic interactions. Magnetic ion concentrations are typically similar in the crystalline and amorphous systems (5–15 at. %) but the differences in structural order cause the relevant electron concentrations to be very different, causing quite different effects. The critical concentration at which the MIT occurs is much greater in amorphous materials due to the increased disorder (atomic concentrations of dopant ions of  $\sim 10$ –15 at. %) compared to their crystalline counterparts (typically 3–4 orders of magnitude smaller). This large difference in dopant concentration lends itself to the study of the critical region proximal to the MIT, because the large number of dopants, which each con-

tribute charge carriers to the system, leads to much larger Fermi energy  $E_F$  for these systems. Experimentally, this means that one can probe the critical dynamics of the system to higher energy scales, both in temperature and frequency domains.<sup>6</sup>

There are several outstanding questions concerning the remarkable magnetic and magnetotransport properties observed in *a*-Gd-Si. Among these are (1) what sets the energy scale below which the magnetic moments influence the properties? From room temperature down to a characteristic temperature  $T^*$ , the properties of *a*-Gd-Si and its nonmagnetic counterpart *a*-Y-Si are nearly identical; below  $T^*$ , the presence of Gd causes strong localization of carriers and large MR. Since the low temperature properties (density of states, conductivity, and optical absorption) of *a*-Gd-Si are well described by MIT theory on each side of the transition, with very few field-dependent parameters, should one consider  $T^*$  as a temperature at which a mass renormalization of carriers by magnetic interactions with local moments occurs, similar to a Kondo-like effect? (2) Why do the high-field magnetization curves  $M(H, T)$  show almost no signature of the MIT, despite the fact that the interactions seemingly must be mediated by conduction electrons (since direct exchange of Gd *f* electrons are negligible at the interdopant distances of samples close to the MIT), but the initial magnetic susceptibility,  $\chi(T)$ , shows a clear signature of the MIT above the spin-glass freezing temperature.  $\chi(T)$  in *a*-Gd-Si is well described by a Curie-Weiss law with nearzero  $\theta$ , a strong dependence on Gd concentration, and an effective moment near but not quite that of the expected  $\text{Gd}^{3+}$  moment, which is quite different behavior from that seen in other MIT systems.

Gadolinium is a rare-earth metal with an atomic configuration of  $4f^7 5d^1 6s^2$ . It is virtually always trivalent, resulting in a  $\text{Gd}^{3+}$  ion which has a well-shielded, half-filled  $4f^7$  shell, which gives a large local moment ( $J=S=7/2$  and  $L=0$ ). The three outer electrons act as donor electrons in the amorphous Si matrix (as evidenced by a negative Hall coefficient and thermopower) and form a dopant band in the band gap of the semiconductor matrix. We have shown in *a*-Gd-Si that both  $T^*$  and MR (at fixed  $T$ ,  $\Delta H$ ) decrease with increasing Gd concentration, while the spin-glass freezing temperature  $T_f$  increases.<sup>7-9</sup> The latter is expected, since increasing Gd concentration leads to stronger Gd-Gd magnetic interactions. The former is, however, surprising and can only be explained by the increased number of electrons with increasing Gd content which we have suggested leads to screening of the magnetic moments.<sup>14</sup> This behavior is opposite to what is expected from Kondo physics, which is in any case not expected to play a role in these systems, since the Gd *f* levels are far from the Fermi energy and is also opposite to the observed increase in  $T_C$  in GaMnAs with increasing Mn doping.<sup>10</sup> Addition of the nonmagnetic ion Y (atomic configuration  $4d^1 5s^2$ , also virtually always trivalent), while holding the Gd concentration constant, increases the conductivity as expected, but also causes a sharp decrease in  $T^*$ .<sup>7</sup> Previous work has investigated the effect of substituting a different rare earth ion (Tb) for Gd in *a*-Si.<sup>11</sup> This system has a large negative MR, similar to but slightly smaller than *a*-Gd-Si with more complex magnetic behavior due to the nonzero orbital moment of Tb, which results in strong randomly oriented local magnetic anisotropy.

TABLE I.  $n_{\text{Gd}}$  for *a*- $\text{Gd}_x\text{Ge}_{1-x}$ , obtained using RBS. Values for  $x$  and  $n_{\text{Gd}}$  are  $\pm 5\%$ . The third column shows  $p_{\text{eff}}$  per Gd as determined from Curie-Weiss fits. However, as discussed in the text, the Bhatt Lee form for  $\chi$  fits the data much better.

Composition $x$	$n_{\text{Gd}}$ (Gd atoms/cm <sup>3</sup> )	$P_{\text{eff}}$ ( $\mu_B/\text{Gd}$ )
0.086	$3.7 \times 10^{21}$	6.28
0.117	$4.9 \times 10^{21}$	5.86
0.127	$5.4 \times 10^{21}$	
0.134	$5.5 \times 10^{21}$	6.14
0.146	$6.1 \times 10^{21}$	4.63
0.154	$6.5 \times 10^{21}$	
0.163	$6.7 \times 10^{21}$	6.10
0.194	$7.9 \times 10^{21}$	5.66
0.254	$1.0 \times 10^{22}$	6.34

The recent reports of Curie temperatures above 100 K in crystalline  $\text{Mn}_x\text{Ge}_{1-x}$  make the study of alternate magnetic dopants in a Ge matrix all the more important.<sup>12</sup> With the goal of obtaining a better understanding of the effects of incorporating magnetic moments into an alternate amorphous semiconducting matrix (with significantly different band gaps and consequently different dielectric constants and electron screenings), *a*- $\text{Gd}_x\text{Ge}_{1-x}$  films were prepared and their magnetic and magnetotransport properties have been studied. In the amorphous alloys, unlike the results obtained by substituting the rare earth (Tb for Gd), very large and systematic changes are found with the change of semiconductor. These differences support the suggestion that electron screening plays a dominant role in determining the energy scale for the effect of magnetic moments and offers a tunable parameter, namely, the band gap of the semiconducting matrix, which determines the onset temperature for the very large obtained MR in these systems.

## II. EXPERIMENT

Thin film samples were prepared by electron-beam co-evaporation under ultrahigh-vacuum growth conditions ( $P < 10^{-9}$  Torr) onto various substrates, depending on the desired measurement constraints and requirements. Rutherford backscattering spectroscopy (RBS) was used to determine the film compositions. Samples were grown from 100 to 400 nm in thickness, and the actual thicknesses were determined by profilometry. The compositions, atomic number density, and the susceptibility per Gd  $p_{\text{eff}}$  (as determined from Curie-Weiss fits) for the samples described here are shown in Table I. ( $\chi$  values for the  $x=0.127$  and  $x=0.154$  samples were not measured.)

Previous high-resolution cross-sectional transmission electron microscopy (XTEM), x ray, and extended x-ray fine structure (XAFS) analysis of *a*-Gd-Si had shown an amorphous structure with no clustering of Gd up to approximately 25 at. % (XAFS specifically showed Gd surrounded entirely by Si nearest neighbors, consistent with density functional analysis).<sup>13</sup> Both x-ray and TEM diffractions confirm the

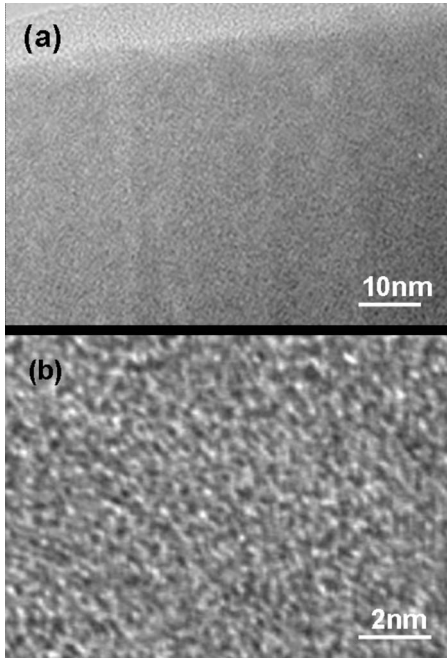


FIG. 1. XTEM micrographs of  $a\text{-Gd}_{0.146}\text{Ge}_{0.854}$ . (a) Low magnification and (b) high-resolution micrographs show the microstructure of the film to be amorphous.

amorphous nature of the  $a\text{-Gd-Ge}$  films. The results of XTEM observations, both at low and high magnifications, for  $a\text{-Gd}_{15}\text{Ge}_{85}$  are shown in Fig. 1. The low-resolution micrograph in Fig. 1(a) shows a slightly columnar morphology with column widths between 11 and 18 nm, as was seen previously in  $a\text{-Gd-Si}$ .<sup>14</sup> This type of structure is commonly seen in vapor-deposited amorphous films (a remnant of diffusion-limited aggregation effects). Figure 1(b) is a high-resolution XTEM micrograph, which shows the film to be primarily amorphous with some hints of lattice fringes visible in very few places. In previous work on  $a\text{-Gd-Si}$ , these fringes were found to become more prominent with increasing Gd concentration and become distinct above  $\sim 25$  at. %, indicative of clustering at higher concentrations (although still a small fraction of the film). This clustering at high dopant concentrations leads to a peak in the dc conductivity as a function of Gd composition.<sup>14</sup> For the current purposes of studying magnetization and transport proximal to the MIT in either  $a\text{-Gd-Si}$  or  $a\text{-Gd-Ge}$ , this value gives an upper cut-off to the range of dopant concentrations to be discussed.

### A. Magnetic susceptibility and magnetization

The ac,  $\chi_{ac}(T)$ , and dc,  $\chi_{dc}(T)$ , susceptibilities and dc magnetization  $M(H, T)$  measurements were performed using a superconducting quantum interference device magnetometer.  $\chi_{ac}(T)$  was measured in an alternating field with a magnitude of 4 or 5 Oe (typically both were measured and compared) at a frequency of 135 Hz.  $\chi_{dc}(T)$  was measured in an applied field of 500 Oe, either after cooling from room temperature in zero applied field, referred to as zero-field cooled (ZFC), or in 500 Oe field, referred to as field cooled (FC). This large

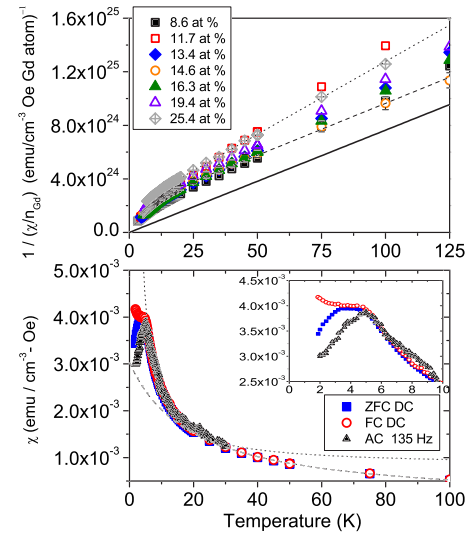


FIG. 2. (Color online) (a) Inverse dc magnetic susceptibility per Gd atom  $1/(\chi_{dc}/n_{\text{Gd}})$  vs  $T$ . Measurement taken at a field of 500 Oe. Solid line shows Curie-Law for non interacting Gd moments. (b)  $\chi_{dc}$  vs  $T$  for  $x=0.146$ .  $\chi_{dc}$  was measured at 500 Oe, applied on warming after cooling in zero field (ZFC) or cooling in field (FC). ac magnetic susceptibility  $\chi_{ac}$  was measured with a driving amplitude of 3 Oe at frequency 135 Hz. Dashed lines in both figures show high temperature Curie-Weiss fits and dotted lines show low temperature Curie-Weiss fits.

field was chosen because the signal for these samples was small and  $M(H)$  was experimentally found to be linear up to 500 Oe. The background signal (including substrate,  $a\text{-Si}$  matrix, and magnetometer) was determined by fitting  $\chi_{dc}$  vs  $1/T$  and taking the intercept as  $1/T$  approaches 0. This background is subtracted from the data shown in Fig. 2.

Figure 2(a) shows the inverse dc susceptibility  $(\chi_{dc})^{-1}$  above the spin-glass freezing  $T_f$  normalized to the number density of Gd atoms  $n_{\text{Gd}}$  (as determined by RBS) for  $a\text{-Gd}_x\text{Ge}_{1-x}$  for  $0.086 < x < 0.254$ . The figure also shows the Curie law dependence for noninteracting Gd moments (solid line). All data lie above this line, meaning that  $\chi(T)$  for all samples is significantly suppressed (factor of 2) below the noninteracting limit.  $\chi_{ac}(T)$  and both FC and ZFC  $\chi_{dc}(T)$  for  $x=0.146$  are shown in Fig. 2(b). These data show the characteristic peak splitting associated with spin-glass freezing, as seen in  $a\text{-Gd-Si}$ .<sup>15-17</sup> For a spin glass, one can typically fit  $\chi(T)$  in the paramagnetic state above  $T_f$  using a Curie-Weiss dependence,

$$\chi = A/(T - \theta), \quad (1)$$

where  $\theta$  is a measure of the strength of the *net* interactions,  $A = n_{\text{Gd}} p_{\text{eff}}^2 \mu_B$ , and the effective moment  $p_{\text{eff}}^2 = g^2 J(J+1)$  is close to the expected single ion value. This mean-field fit is valid for the low-field  $\chi$  for spin glasses such as Cu-Mn and  $a\text{-Gd-Si}$  above  $T_f$ .<sup>15,16</sup> For other Gd-based spin glasses, it is common to find large positive  $\theta$  and effective moments which are slightly increased above the expected value of  $7.9 \mu_B/\text{Gd}$ . What was found instead for  $a\text{-Gd-Si}$  is a good Curie-Weiss fit with  $\theta$  near zero ( $\ll T_f$ ), and an effective mo-

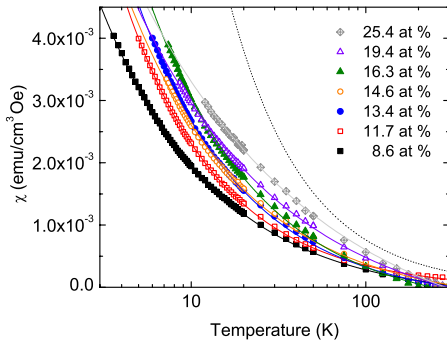


FIG. 3. (Color online) Susceptibility of *a*-Gd-Ge plotted vs temperature. The fits are to the Bhatt-Lee form:  $A'/T^\alpha$ . We found  $\alpha \approx 0.7$  and  $A'$  increased monotonically with  $x$ , unlike *a*-Gd-Si. The dotted line shows the Curie-weiss law susceptibility for noninteracting Gd in Ge at 14.5 at. % doping concentration.

ment which was close to but smaller than  $7.9\mu_B$ , and depending strongly on composition with a large peak at the MIT.<sup>15</sup>

The Curie-Weiss form of Eq. (1) for *a*-Gd-Ge does not fit the measured  $\chi(T)$  above  $T_f$  very well at all, unlike what was seen in *a*-Gd-Si. Fits to both low and high temperatures, using Eq. (1), are shown in Fig. 2(a). Moreover, even a qualitative fit yields an effective moment which is much smaller than the expected effective moment of  $7.9\mu_B$  [the values of the effective moments  $p_{eff}$  as determined from qualitative fits of Eq. (1) between  $T_f$  and 300 K are summarized in Table I]. In the *a*-Gd-Ge samples studied here, the susceptibility per Gd moment also shows no significant dependence on composition. The 14.6 at. % sample has a lower value of susceptibility per Gd moment than the other samples. Though this is intriguing because 0.146 corresponds to the critical concentration at which the metal-insulator transition occurs in this amorphous metal-semiconductor system, this value does not fall significantly outside the margin of error for these results and further more accurate measurements would be needed to confirm this result. This concentration independence is unlike the strong (factor of 2) dependence on the rare-earth concentration seen previously, including a clear peak observed at the MIT in *a*-Gd-Si, the ternary alloys *a*-Gd-Y-Si, and *a*-Tb-Si.  $\chi(T)$  for *a*-Gd<sub>*x*</sub>Ge<sub>1-*x*</sub> was instead fitted to a power law,

$$\chi = A'/T^\alpha \quad (2)$$

[Eq. (2) will be referred to as the Bhatt-Lee model].<sup>18</sup> This Bhatt-Lee model fit has been used for the singly occupied states found in the crystalline doped semiconductor system Si:P near the MIT and a similar power law behavior (with  $\alpha \approx 0.5$  and  $A' < 0$ ) has been used in strongly correlated *f*-electron materials displaying non-Fermi liquid behavior.<sup>19-22</sup> This form fits the *a*-Gd-Ge data remarkably better than the Curie-Weiss law (as shown in Fig. 3) for  $T$  from 300 K to  $T_f$  with  $\alpha \approx 0.75$  for all  $x$ , and  $A'$  monotonically dependent on  $x$ .

Magnetization  $M$  was also measured at various  $T$  as a function of applied magnetic field  $H$  for various  $x$ . The data are shown in Fig. 4 for  $x=0.14$  for *a*-Gd-Ge at a series of

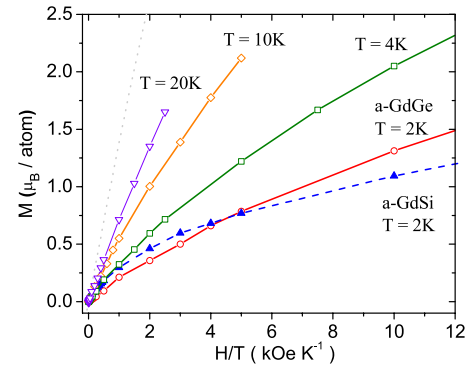


FIG. 4. (Color online) Magnetic moment per Gd atom vs ratio of applied field  $H$  to temperature  $T$ . Both samples are  $x=0.14$ . Dotted line is the calculated Brillouin function for noninteracting Gd. *a*-Gd-Si data (dashed line) is shown for 2 K only, and the data for *a*-Gd-Ge (solid lines) are shown for 2, 4, 10, and 20 K.

temperatures from 2 to 20 K.  $M$  vs  $H/T$  data for a 14 at. % *a*-Gd-Si sample is shown for comparison. These magnetization curves are shown as the moment per Gd atom vs the ratio of the applied field to the temperature ( $M/n_{Gd}$  vs  $H/T$ ). The dotted line is the calculated Brillouin function for noninteracting Gd moments, which rises rapidly for small values of  $H/T$  and eventually saturates at  $7.9\mu_B$ . The strong suppression below the Brillouin function is evidence of the strength of antiferromagnetic Gd-Gd interactions, consistent with the observed spin-glass freezing, which were previously seen in *a*-Gd-Si. These antiferromagnetic interactions were found to suppress  $M$  below the saturation magnetization value even at fields as large as 25 T.<sup>23</sup> A close inspection of the 2 K data for *a*-Gd-Ge reveals that the initial low-field response to an applied field is suppressed below that of *a*-Gd-Si, and is also well below the Brillouin function. This behavior indicates that although both systems show significant low-field Gd-Gd interactions, the interaction strength between the Gd moments at these initial low fields is stronger in *a*-Gd-Ge as compared to *a*-Gd-Si. However, at the highest measured  $H$  and lowest measured  $T$  ( $H/T=25$ ), although  $M$  for both *a*-Gd-Si and *a*-Gd-Ge fall well below the nearly saturated magnetization of the Brillouin function, the response of *a*-Gd-Ge is a factor of  $\sim 1.5$  greater than *a*-Gd-Si, indicating that the magnetic interaction strength between Gd moments at high fields is weaker in *a*-Gd-Ge than in *a*-Gd-Si.

## B. Electrical conductivity and magnetoconductivity

dc conductivity,  $\sigma_{dc}(T)$ , measurements were performed on samples lithographically patterned to give a well-defined geometry. A standard four-probe technique was used and measurements were taken for all samples from  $4 < T < 300$  K and for selected samples to 300 mK.  $\sigma(T)$  increases steadily both with increasing temperature and with increasing Gd concentration, as illustrated in Fig. 5. This behavior follows the trend from previous studies of *a*-Gd-Si and other amorphous rare earth-silicon and metal-silicon alloys. The critical concentration  $x_C$  separating a metallic ground state from an

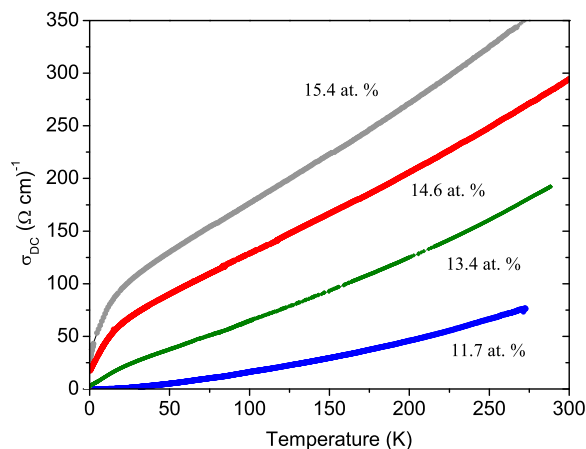


FIG. 5. (Color online)  $\sigma(T)$  for a series of  $a\text{-Gd}_x\text{Ge}_{1-x}$  for  $0.117 \geq x \leq 0.154$ .

insulating one is near 14 at. %, identical to that found in  $a\text{-Gd-Si}$  and in the nonmagnetic analog  $a\text{-Y-Si}$ .<sup>7</sup> The definition metallic or insulating refers here to the  $T=0$  K residual conductivity; metallic samples having a finite residual conductivity at 0 K and insulating samples extrapolating to infinite resistance at 0 K (this being the criterion that defines the MIT in disordered electronic systems). The number density  $n_{\text{Gd}}$  in  $a\text{-Gd-Si}$  is nearly 20% larger than in  $a\text{-Gd-Ge}$  (see Table I) so it is interesting to note that  $x_C$  is the same. It should also be noted that  $x_C$  in  $a\text{-Nb-Si}$  occurs at 11.5 at. % Nb, suggesting that both valency and atomic radius play a role in determining  $x_C$ .<sup>24</sup>

Figure 5 shows a comparison of  $\sigma(T)$  for samples on both the metallic side of the MIT ( $x > x_C$ ) and on the insulating side. These thin film samples are all thick enough (100–400 nm) to be considered as three-dimensional (3D) systems. The theoretical form that describes  $\sigma(T)$  for metallic samples in 3D disordered electronic systems is given by

$$\sigma_{dc}(T) = \sigma_0 + AT^{1/2} + BT, \quad (3)$$

where  $\sigma_0$  is the conductivity at  $T=0$ . The  $T^{1/2}$  term stems from correlation effects and the resulting Coulomb gap in the electron density of states (DOS), and the term with the linear temperature dependence is due to quantum backscattering effects in the presence of inelastic electron-electron scattering in three dimensions.<sup>25</sup> This form of the temperature dependence has been shown to fit the nonmagnetic  $a\text{-Y-Si}$   $\sigma(T)$  over an extraordinarily wide temperature range (0.1–300 K). For samples on the insulating side of the MIT and at sufficiently low temperature,

$$\sigma_{dc}(T) \propto \exp[T_0/T]^{-1/\beta}, \quad (4)$$

with  $\beta=2$  for variable range hopping (VRH) in the presence of a Coulomb gap, indicative of strong electron-electron interactions in the system or  $\beta=4$  (in three dimensions) for VRH excitations that extend beyond the Coulomb gap.<sup>26,27</sup> This dependence breaks down at higher temperatures ( $>50$  K), presumably due to the onset of other conduction processes, causing  $\sigma(T)$  for samples which are insulating at

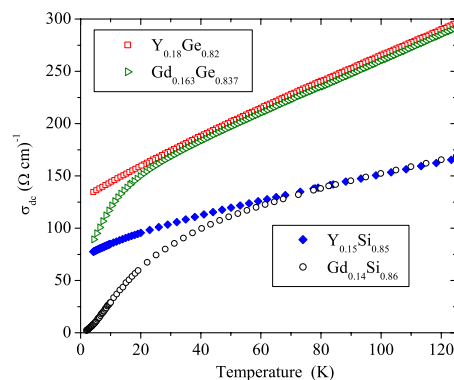


FIG. 6. (Color online)  $\sigma(T)$  for comparable  $a\text{-Y-Si}$  and  $a\text{-Gd-Si}$  as well as comparable  $a\text{-Y-Ge}$  and  $a\text{-Gd-Ge}$  samples. The conductivity of both Gd alloys drops sharply at low temperatures as compared to their nonmagnetic yttrium-doped analogs.  $T^*$  is visible as the break between the curves and is 60 and 20 K for  $a\text{-Gd-Si}$  and  $a\text{-Gd-Ge}$ , respectively, here.

low  $T$  to follow nearly parallel curves to the metallic samples at higher  $T$ , as seen in Fig. 6.

Previous studies on  $a\text{-Gd-Si}$  and the nonmagnetic analog  $a\text{-Y-Si}$  have shown that the two have nearly identical  $\sigma(T)$  above a characteristic temperature  $T^*$  and that  $\sigma(T)$  above  $T^*$  is readily described by Eq. (2), showing a strong linear dependence on  $T$ .<sup>7</sup> Below  $T^*$ ,  $a\text{-Y-Si}$  continues to fit the model, whereas  $\sigma(T)$  for  $a\text{-Gd-Si}$  drops sharply. This behavior is also seen in a comparison of  $\sigma(T)$  for  $a\text{-Gd-Ge}$  and  $a\text{-Y-Ge}$ , as shown in Fig. 6. The relatively sharp break in  $\sigma(T)$  seen below  $\sim 50$  K is an indication of the onset of the localizing effects of the magnetic Gd ions on the itinerant electrons, as previously seen in  $a\text{-Gd-Si}$ .  $T^*$  is a strong function of composition and has surprisingly been found to decrease sharply with increasing  $x$ .<sup>7</sup> This characteristic magnetic temperature  $T^*$  of  $a\text{-Gd-Ge}$  is also significantly lower than that of  $a\text{-Gd-Si}$  at similar concentrations, an effect that we suggest is due to the smaller band gap and consequently increased electron screening for Ge compared to Si. On the insulating side of the MIT, the presence of the magnetic Gd ions presumably has a similar effect on  $\sigma(T)$  at low temperatures. However, our inability to fit  $\sigma(T)$  over the necessary temperature range spanning  $T^*$  (above 30 K) has made it impossible to define  $T^*$  for insulating samples.

We now turn to the magnetoconductance (MG) of these samples, where  $\text{MG} = [\sigma(H) - \sigma(0)] / \sigma(0)$ . (Note that  $\text{MG} = -\text{MR}$ ). The dc conductivity of  $a\text{-Gd-Ge}$  and  $a\text{-Gd-Si}$  at low temperatures increases in a magnetic field, i.e., these materials show negative MR. Figure 7 shows  $\sigma(T)$  for  $a\text{-Gd}_{0.134}\text{Ge}_{0.864}$ , an insulating sample, at various fields. The transport is similar to that seen in insulating  $a\text{-Gd-Si}$  samples, showing typical VRH behavior. The transport data in Fig. 7 is plotted as a function of  $T^{-1/2}$  to highlight the temperature range over which VRH at energies smaller than the Coulomb gap would occur. However, the data are not linear over any extended temperature range indicative of the fact that the crossovers between the various temperature ranges for different thermally assisted hopping behaviors are not sharp (unlike insulating samples of  $a\text{-Gd-Si}$  where the curves fit well).<sup>28</sup>

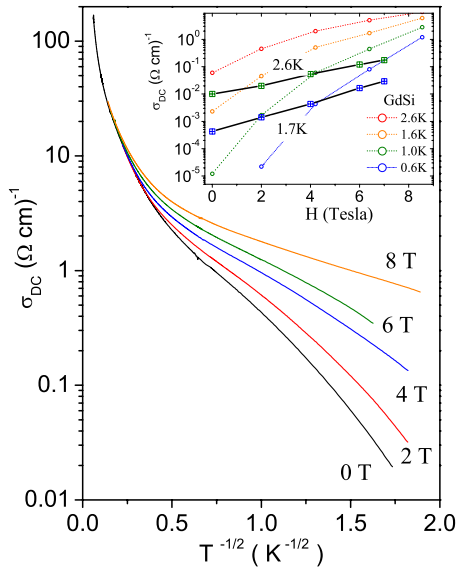


FIG. 7. (Color online)  $\sigma(T)$  at various  $H$  for  $x=0.134$   $a\text{-Gd}_x\text{Ge}_{1-x}$  sample. Inset shows a comparison of isotherms for a 0.13  $a\text{-Gd}_x\text{Si}_{1-x}$  sample (dotted lines) and  $x=0.127$   $a\text{-Gd}_x\text{Ge}_{1-x}$  sample (solid lines).

The dc conductivity at 8 T grows to over 1 order of magnitude greater than the zero-field conductivity for  $T < 4$  K, as seen in Fig. 7. This impressive negative MR is, however, dwarfed by the over 4 orders of magnitude change in MR measured previously for a similar concentration  $a\text{-Gd-Si}$  sample.<sup>29</sup> No theoretical model to date has yet been able to describe these effects observed now in both  $a\text{-Gd-Ge}$  and  $a\text{-Gd-Si}$ . The dc conductivity of  $a\text{-Gd-Ge}$ , in any applied field, approaches the zero-field conductivity at higher temperatures ( $T > 20$  K), indicating that the magnetic moments of the Gd atoms significantly affect the conductivity only at low temperature. This trend is consistent with the magnetization results of Fig. 4, namely, that the Gd-Gd magnetic interactions seem to turn on at lower temperature (which is a strong indication that the Gd-Gd interaction is an indirect, carrier-mediated one). The MG is far more dramatic in  $a\text{-Gd-Si}$  than in  $a\text{-Gd-Ge}$ , as seen in the inset of Fig. 7, which shows a comparison of isotherms of MG data for the previously measured 13 at. %  $a\text{-Gd-Si}$  sample and for the 12.7 at. %  $a\text{-Gd-Ge}$  sample.

The MG decreases dramatically with increasing Gd concentration, as shown in Fig. 8. In this figure, the MG is for an applied field of 6 T. In  $a\text{-Gd-Si}$ , by comparison, for a 14.5 at. % sample, the MG drops below 5% at 40 K, whereas Fig. 8 shows that the 14.6 at. %  $a\text{-Gd-Ge}$  drops below 5% MG closer to 20 K. A small, relatively flat, negative MR tail ( $\sim 1\%$ – $4\%$ ) persists in these  $a\text{-Gd-Ge}$  samples up to  $T > 50$  K. This persistent tail of negative MR, is caused by the magnetic dopant Gd, because MR measurements of a comparably doped  $a\text{-Y-Ge}$  sample shows that the MR from the disordered electronic system alone is positive and much less than 1% above 15 K.<sup>30</sup>

### III. DISCUSSION

In an attempt to understand the differences in magnetic interactions and the possible effects of dopant spacing, we

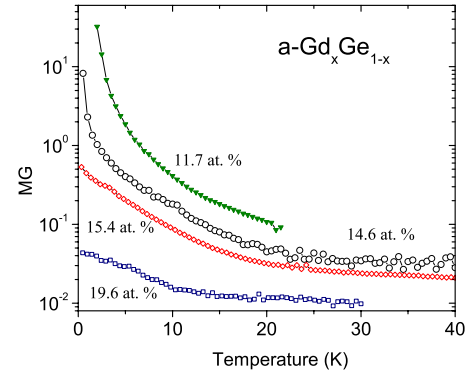


FIG. 8. (Color online) MG for  $a\text{-Gd}_x\text{Ge}_{1-x}$  samples ranging from  $x=0.117$  to 0.196.

analyzed the difference in the average inter-Gd spacing in the two semiconductor matrices. Figure 9 shows a side-by-side comparison of the volume density of the dopant Gd  $n_{\text{Gd}}$  (in atoms/cm<sup>3</sup>) as a function of the RBS-determined Gd atomic density for  $a\text{-Gd-Si}$  and  $a\text{-Gd-Ge}$ . It is surprising to note that each Gd dopant atom in the amorphous silicon matrix is displacing only as much volume as the Si atom it is effectively replacing over the doping range being investigated. This is clearly seen in that the slope of the  $a\text{-Gd-Si}$  data is almost identical to the volume density of pure silicon ( $5.0 \times 10^{22}$  cm<sup>-3</sup>). By comparison, Gd incorporated into the  $a\text{-Ge}$  matrix causes the atomic number density to decrease below that of pure  $a\text{-Ge}$  (pure  $a\text{-Ge}$  has an atomic density of  $4.3 \times 10^{22}$  cm<sup>-3</sup> and the slope for the  $a\text{-Gd-Ge}$  data in Fig. 9 is  $4.0 \times 10^{22}$  cm<sup>-3</sup>).<sup>31</sup> However, at any measured Gd atomic number density, for  $a\text{-Gd-Ge}$ , the volume density is lower than in  $a\text{-Gd-Si}$ , indicating that the Gd dopants are more distal from each other in the Ge matrix. At these distances, direct exchange does not play any significant role. However, the larger distance between Gd atoms in the Ge matrix has still the effect of suppressing the strength of the overall indirect carrier-mediated Ruderman-Kittel-Kasuya-Yosida (RKKY) type magnetic interactions. We note that in amorphous systems, the wave vector  $k$  is not well defined, so a

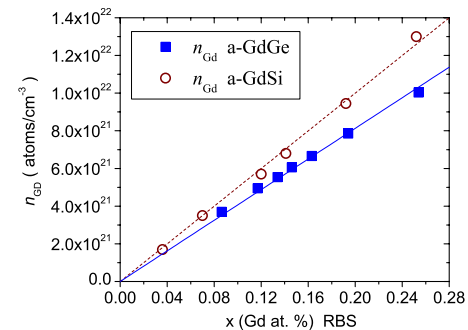


FIG. 9. (Color online) Volume density  $n_{\text{Gd}}$  vs atomic percent  $x$  of gadolinium. The slopes indicate the density at which Gd is going into the matrix. For  $a\text{-Gd-Si}$ , the slope of  $5.0 \times 10^{22}$  cm<sup>-3</sup> is identical to the volume density of  $a\text{-Si}$ . The slope for  $a\text{-Gd-Ge}$  is  $4.0 \times 10^{22}$  cm<sup>-3</sup>, indicating a denser alloy than the volume density of pure  $a\text{-Ge}$  ( $3.25 \times 10^{22}$  cm<sup>-3</sup>).

rigorous application of the RKKY theory is inappropriate. However, we argue that an RKKY-type magnetic interaction still exists as both local magnetic moments and itinerant electrons are present in both the metallic and even the insulating systems at finite temperatures. The RKKY indirect exchange mechanism between Gd atoms can be written as

$$J_{\text{Gd-Gd}}(r) = 6\pi Z J_{sf}^2 N(E_F) \left( \frac{\sin(2k_F r)}{(2k_F r)^4} - \frac{\cos(2k_F r)}{(2k_F r)^3} \right), \quad (5)$$

where  $Z$  is the number of conduction electrons per atom,  $J_{sf}$  the  $s$ -conduction electron Gd  $f$ -shell electron exchange constant,  $N(E_F) \propto n_{\text{Gd}}^{1/3}$  the DOS at the Fermi energy,  $r \propto n_{\text{Gd}}^{-1/3}$  the interparticle distance, and  $k_F \propto n_{\text{Gd}}^{1/3}$  the Fermi wave vector.<sup>16</sup> For equivalent atomic doping concentration  $x$ ,  $n_{\text{Gd}}$  is smaller in the Ge system as compared to the Si matrix. From Eq. (5), we see that the term in parentheses is independent of  $n_{\text{Gd}}$ . However, the reduced  $N(E_F)$  term will result in an overall weaker net magnetic interaction in Ge. Both the Anderson and Kondo models, which are used to describe interactions between local magnetic moments and conduction electrons, lead to a functional form for  $J_{sf} \propto U$ , where  $U$  is the Coulomb interaction energy. Although typically taken as an on-site interaction,  $U$  may be partially screened by the local environment, namely, the semiconductor matrix. Thus, in certain instances, even the  $J_{sf}$  term may be smaller in  $a$ -Gd-Ge than in  $a$ -Gd-Si. Either of the above-mentioned effects lead to a weaker  $J_{\text{Gd-Gd}}$ , which in turn would be manifest as a slightly suppressed spin-glass freezing temperature  $T_f$ . In Fig. 2, the cusp in  $\chi_{ac}$  is a good indicator of  $T_f=5$  K for the 14.6 at. %  $a$ -Gd-Ge sample. In  $a$ -Gd-Si, for 14 at. %, the cusp in  $\chi_{ac}$  taken under the same conditions (135 Hz and 4 Oe) occurs at  $T_f=6$  K. Although this is a small difference, the shift is consistent with the expectation that the indirect carrier-mediated magnetic interactions are weaker in  $a$ -Gd-Ge than in  $a$ -Gd-Si.

The magnetic susceptibility data shown in Fig. 2 was analyzed in terms of a Curie-Weiss law and as can be seen in the figure, the fits to the high and low temperature data differ significantly. However, a general trend in the susceptibility data for all of the measured  $a$ -Gd-Ge samples was that the value of  $\theta$  from Eq. (1) was slightly negative for the high temperature fits and crossed over to slightly positive for the low temperature fits. This suggests a stronger net negative exchange at lower temperatures. However, the Curie-Weiss law fit well and  $\theta$  was consistently near zero in  $a$ -Gd-Si, and this suggests that the balance of ferromagnetic and antiferromagnetic interactions is dependent on the different relative spacings of the dopant Gd atoms in the Ge matrix.

The suppressed moment per Gd atom in  $a$ -Gd-Ge (as determined from the Curie-Weiss fitting) and the fact that  $\chi$  actually fits better to the Bhatt-Lee form of magnetic susceptibility,  $A'/T^\alpha$ , are intriguing but unexplained. This latter form for the magnetic susceptibility stems from a model that has spin 1/2 moments pairing and forming spin singlets, thus dropping out of the net moment of the system (i.e., in Si:P the extra electrons from the P dopants pair antiferromagnetically). However, it is difficult to believe that this could be occurring in the Gd-doped system simply because each Gd

contributes spin 7/2 (although neighboring Gd atoms might still pair up antiferromagnetically). For Si:P, with spin 1/2, this form for the susceptibility is easily obtained from the microscopic system, and this same form may be possible for magnetic dopant of higher spins depending on the form of exchange in the Hamiltonian.<sup>32</sup>

In heavy fermion non-Fermi liquid (NFL) systems, both in systems with transition metal magnetic dopants ( $d$  shell) and rare earth magnetic elements ( $f$ -shell), a power law behavior of the magnetic susceptibility due to electronic correlation effects is also found. This shift in  $\chi$  is an effective enhancement of the total response to an applied field above a Curie-Weiss law occurring below the Kondo temperature (as the electrons polarize). In these NFL systems, it is typically found that  $\chi(T) = \chi(0)[1 - c(T/T_K)^{1/2}]$ , where  $T_K$  is the Kondo temperature.<sup>20</sup> A Curie-Weiss fit of the high temperature  $a$ -Gd-Ge data is shown as a dashed line in Fig. 2(b). The low temperature susceptibility is then seemingly enhanced above that of the Curie-Weiss law, similar to that observed in NFL systems. However, the deviation does not fit a  $T^{1/2}$  dependence as in NFL systems, and the total high temperature magnetization of these thin  $a$ -Gd-Ge films used to determine  $\chi$  is quite small, leading to significant error from a Curie-Weiss fit of the high temperature data alone.

The Bhatt-Lee theory predicts full scaling of magnetization data and the theory has been verified by successful scaling analysis of Si:P and Si:B near the MIT.<sup>33,34</sup> As mentioned above, these doped semiconductor systems fit the susceptibility given by Eq. (2). For magnetization data taken at various temperatures and/or fields, when plotted as  $(M/T\chi)$  versus  $H/T$ , the data for these crystalline doped semiconductors collapse onto a single curve. In an attempt to verify whether this model might be correct for  $a$ -Gd-Ge, we attempted a similar scaling analysis. However, although the susceptibility for our  $a$ -Gd-Ge samples seems to be well described by the Bhatt-Lee susceptibility of Eq. (2), attempts to scale the magnetization data were unsuccessful. In particular, we measured  $M$  vs  $H$  at various temperatures: for any one sample, the data failed to collapse on a single universal curve.

The transport data for  $a$ -Gd-Ge gives two strong indicators that the interactions between the local Gd magnetic moments and the conduction electrons are weaker than in  $a$ -Gd-Si. First, the characteristic temperature  $T^*$ , below which charge localization occurs as compared to the non-magnetic Yttrium-doped analog, is lower in  $a$ -Gd-Ge. Second, the MG observed in  $a$ -Gd-Ge is smaller, both in maximum magnitude and as a function of field.

In summary, we have shown two general trends in magnetic properties of the  $a$ -Gd-Ge samples as compared to the  $a$ -Gd-Si samples. First, the susceptibility per Gd atom in  $a\text{-Gd}_x\text{Ge}_{1-x}$  is suppressed even more so than in  $a\text{-Gd}_x\text{Si}_{1-x}$  with no significant dependence on composition for  $x$  near the MIT. Second, the high-field magnetization curves are well below the Brillouin function, indicating the presence of antiferromagnetic interactions, with  $a$ -Gd-Ge displaying stronger low-field interactions, but weaker high field interactions, as compared to  $a$ -Gd-Si. The suppression of the magnetization below the Brillouin function is a more significant result since the Curie-Weiss law is one limiting case of the Brillouin function. The overall weaker magnetic moment-

conduction electron interaction is highlighted in the much lower characteristic temperature at which magnetic interactions turn on causing the dc conductivity to deviate from a nonmagnetic analog; namely,  $T^*$  is lower in *a*-Gd-Ge than in *a*-Gd-Si. For a given concentration, we found no indication at  $T^*$  of an anomaly in the susceptibility data.  $T^*$  probes the zero-field magnetic moment-conduction electron effects. However, the magnetoconductance effects of Gd doped into the Ge matrix, measured in this work up to 8 T, are also less dramatic than for their Si counterparts. This then conclusively demonstrates that the matrix and the tuning of the host matrix band gap plays a significant role in setting the energy

scale below which magnetic moments influence the properties of the system.

#### ACKNOWLEDGMENTS

We thank R. Bhatt for useful discussions. We acknowledge use of facilities in the John M. Cowley Center for High Resolution Electron Microscopy at Arizona State University, and we thank Bob Culbertson and Barry Wilkens for assistance with RBS. This research was supported by the NSF DMR-0505524 and DMR-0203907.

\*helgren@berkeley.edu

†lzensg@ucsd.edu

<sup>1</sup>H. Ohno, *Science* **281**, 951 (1998).

<sup>2</sup>T. Dietl, H. Ohno, F. Matsukura, J. Cibert, and D. Ferrand, *Science* **287**, 1019 (2000).

<sup>3</sup>K. R. Kittilstved, N. S. Norberg, and D. R. Gamelin, *Phys. Rev. Lett.* **94**, 147209 (2005).

<sup>4</sup>C. H. Patterson, *Phys. Rev. B* **74**, 144432 (2006).

<sup>5</sup>I. Zutic, J. Fabian, and S. Das Sarma, *Rev. Mod. Phys.* **76**, 323 (2004).

<sup>6</sup>E. Helgren, L. Zeng, K. Burch, D. Basov, and F. Hellman, *Phys. Rev. B* **73**, 155201 (2006).

<sup>7</sup>E. Helgren, J. J. Cherry, L. Zeng, and F. Hellman, *Phys. Rev. B* **71**, 113203 (2005).

<sup>8</sup>B. L. Zink, V. Preisler, D. R. Queen, and F. Hellman, *Phys. Rev. B* **66**, 195208 (2002).

<sup>9</sup>F. Hellman, M. Q. Tran, A. E. Gebala, E. M. Wilcox, and R. C. Dynes, *Phys. Rev. Lett.* **77**, 4652 (1996).

<sup>10</sup>T. Jungwirth, J. Masek, K. Y. Wang, K. W. Edmonds, M. Sawicki, M. Polini, J. Sinova, A. H. MacDonald, R. P. Campion, L. X. Zhao, N. R. S. Farley, T. K. Johal, G. van der Laan, C. T. Foxon, and B. L. Gallagher, *Phys. Rev. B* **73**, 165205 (2006).

<sup>11</sup>M. Liu and F. Hellman, *Phys. Rev. B* **67**, 054401 (2003).

<sup>12</sup>Y. D. Park, A. T. Hanbicki, S. C. Erwin, C. S. Hellberg, J. M. Sullivan, J. E. Mattson, T. F. Ambrose, A. Wilson, G. Spanos, and B. T. Jonker, *Science* **295**, 651 (2002).

<sup>13</sup>D. Haskel, J. W. Freeland, J. Cross, R. Winarski, M. Newville, and F. Hellman, *Phys. Rev. B* **67**, 115207 (2003).

<sup>14</sup>E. Helgren, D. Queen, F. Hellman, L. Zeng, R. Islam, and David J. Smith, *J. Appl. Phys.* **101**, 093712 (2007).

<sup>15</sup>F. Hellman, D. R. Queen, R. M. Potok, and B. L. Zink, *Phys. Rev. Lett.* **84**, 5411 (2000).

<sup>16</sup>J. A. Mydosh, *Spin Glasses* (Taylor & Francis, London, 1993).

<sup>17</sup>R. N. Bhatt, P. Norblad, and P. Svendlidh, in *Spin Glasses and Random Fields*, edited by A. P. Young (World Scientific, Singapore, 1997).

<sup>18</sup>R. N. Bhatt and P. A. Lee, *Phys. Rev. Lett.* **48**, 344 (1982).

<sup>19</sup>A. Roy and M. P. Sarachik, *Phys. Rev. B* **37**, 5531 (1988).

<sup>20</sup>M. B. Maple, M. C. de Andrade, J. Herrmann, Y. Dalichaouch, D. A. Gajewski, C. L. Seaman, R. Chau, R. Movshovich, M. C. Aronson, and R. Osborn, *J. Low Temp. Phys.* **99**, 223 (1995).

<sup>21</sup>H. von Löhneysen, *J. Phys.: Condens. Matter* **8**, 9689 (1996).

<sup>22</sup>G. R. Stewart, *Rev. Mod. Phys.* **73**, 797 (2001); **78**, 743 (2006).

<sup>23</sup>F. Hellman, W. Geerts, and B. Donehew, *Phys. Rev. B* **67**, 012406 (2003).

<sup>24</sup>G. Hertel, D. J. Bishop, E. G. Spencer, J. M. Rowell, and R. C. Dynes, *Phys. Rev. Lett.* **50**, 743 (1983).

<sup>25</sup>P. A. Lee and T. V. Ramakrishnan, *Rev. Mod. Phys.* **57**, 287 (1985).

<sup>26</sup>N. Mott, *Metal-Insulator Transitions* (Taylor & Francis, London, 1990).

<sup>27</sup>B. I. Shklovskii and A. L. Efros, *Electronic Properties of Doped Semiconductors* (Springer, Berlin, 1984).

<sup>28</sup>E. Helgren, N. P. Armitage, and G. Gruner, *Phys. Rev. B* **69**, 014201 (2004).

<sup>29</sup>P. Xiong, B. L. Zink, S. I. Applebaum, F. Hellman, and R. C. Dynes, *Phys. Rev. B* **59**, R3929 (1999).

<sup>30</sup>E. Helgren, L. Zeng, and F. Hellman (unpublished).

<sup>31</sup>Laaziri, S. Roorda, and J. M. Baribeau, *J. Non-Cryst. Solids* **191**, 193 (1995).

<sup>32</sup>R. N. Bhatt (private communication).

<sup>33</sup>M. P. Sarachik, A. Roy, M. Turner, M. Levy, D. He, L. L. Isaacs, and R. N. Bhatt, *Phys. Rev. B* **34**, 387 (1986).

<sup>34</sup>A. Roy, M. P. Sarachik, and R. N. Bhatt, *Solid State Commun.* **60**, 513 (1986).